Whole Hepatic Lipid Volume Quantification and Color Mapping by Multi-slice and Multi-point Magnetic Resonance Imaging

Hiroyuki Igarashi,[1*] Fumika Shigiyama,[1*] Noritaka Wakui,[2] Hidenari Nagai,[2] Kazutoshi Shibuya,[3] Nobuyuki Shiraga,[4] Takahisa Hirose,[1] Naoki Kumashiro[1]

[1]Division of Diabetes, Metabolism, and Endocrinology, Department of Medicine, Toho University Graduate School of Medicine, Tokyo, Japan

[2]Division of Gastroenterology and Hepatology, Department of Medicine, Toho University Graduate School of Medicine, Tokyo, Japan

[3]Department of Surgical Pathology, Toho University Graduate School of Medicine, Tokyo, Japan

[4]Department of Radiology, Toho University Graduate School of Medicine, Tokyo, Japan

[*]These authors contributed equally to this work.

Corresponding Author:

A/Prof. Naoki Kumashiro, MD, PhD

6-11-1 Omori-Nishi, Ota-ku, Tokyo 143-8541, Japan

Phone: +81-3-3762-4151

Fax: +81-3-3765-6488

E-mail: naoki.kumashiro@med.toho-u.ac.jp

Running head: Whole hepatic lipid volume quantification

Abstract

Aim: Current approaches for hepatic steatosis assess only a small point within the liver and may cause inaccuracy for longitudinal observation. We aimed to establish a reliable non-invasive method for whole hepatic lipid content evaluation.

Methods: Fifty-two subjects having hepatic steatosis underwent liver biopsy. Hepatic lipid content was assessed by Dixon in-phase/out-of-phase magnetic resonance imaging (MRI) and proton magnetic resonance spectroscopy (^{1}H-MRS). Using multi-slice and multi-point MRI, we calculated the lipid intensity of every voxel throughout the liver and show the color-mapped lipid distributions. This new analysis could also quantify the whole hepatic lipid and whole liver volumes absolutely. The diagnostic performance of hepatic lipid content between the new analysis and ^{1}H-MRS methods was compared by receiver operating characteristics (ROC) curve analysis referring to the steatosis scores of the liver biopsy.

Results: Areas under the ROC for the diagnosis of steatosis scores ≥1, ≥2, and ≥3 using MRI and ^{1}H-MRS were 0.86 (95% confidence interval [CI]: 0.70–1.00) and 0.98 (95% CI: 0.93–1.00), 0.94 (95% CI: 0.87–1.00) and 0.93 (95% CI: 0.86–1.00), and 0.95 (95% CI: 0.89–1.00) and 0.97 (95% CI: 0.93–1.00), respectively, showing comparable diagnostic accuracies. However, color mapping showed some inconsistencies between the methods.

Conclusions: We described a non-invasive and repeatable evaluation method of whole hepatic lipid accumulation with absolute quantification and color mapping. Hepatic steatosis was accurately evaluated regardless of heterogeneous lipid accumulation. The whole hepatic lean volume, reflecting hepatic parenchymal condition, can also be determined with this method.

Keywords: hepatic steatosis, liver volume, absolute quantification, hepatic lipid volume, color mapping, magnetic resonance imaging

Introduction

Nonalcoholic fatty liver disease (NAFLD) is a common liver disease with an estimated worldwide incidence of 25%.[1] NAFLD begins with hepatic lipid accumulation that causes insulin resistance and fibrosis and leads to type 2 diabetes, cardiovascular disease, cirrhosis, and hepatocellular carcinoma, which are serious problems for both individuals and societies.[2] Thus, assessment of hepatic lipid accumulation is crucial and essential for the management of patients with NAFLD.

Histological examination of liver specimens is considered the gold standard for the diagnosis of NAFLD.[3] However, liver biopsy is invasive, costly, and difficult to use as a screening tool. In addition to invasiveness, repeating biopsy sampling for the longitudinal monitoring may lead to inaccuracies due to sampling errors associated with uneven hepatic lipid accumulation in patients with NAFLD.[4-6] Thus, alternative imaging techniques have been established to evaluate hepatic steatosis.

Among various imaging techniques, ultrasonography (US) and computed tomography are widely used for screening but are not suitable for quantitative and accurate monitoring. Proton magnetic resonance spectroscopy (^{1}H-MRS) and magnetic resonance imaging (MRI) are common MR-based techniques for hepatic steatosis assessment.[7-10] They can determine the difference in resonance frequencies between water and fat proton signals to quantitatively measure the signal fat fraction and/or the proton density fat fraction (PDFF).[7, 8] MRI fat fraction calculated by the Dixon in-phase and out-of-phase method is one of the established method in evaluating hepatic steatosis.[9, 11-14] In addition, it is proved that hepatic steatosis quantification by MRI is

significantly correlated with liver biopsy assessment, and thus, is reliable.[9] Regarding the ^{1}H-MRS method, numerous studies suggested that the results of ^{1}H-MRS also correlate with those of liver biopsy,[15-19] and ^{1}H-MRS has become a popular alternative non-invasive method.[16-19] Furthermore, recently, the MRI-based PDFF method has also become popular as a reliable quantitative method for clinical trials.[8, 10] Thus, MR-based techniques for hepatic steatosis assessment have become established alternative non-invasive methods.

However, both ^{1}H-MRS and PDFF by MRI methods have a limitation for accuracy in monitoring hepatic steatosis.[20] ^{1}H-MRS acquires signals only from a single and small-sized voxel (typically 2×2×2 cm^3 or 3×3×3 cm^3) on the liver. Similarly, the current PDFF MRI method acquires signals only from a few regions of interest.[9, 10, 13] As lipid accumulation in the liver is usually uneven, these results could be biased due to region selection and thus may not reflect the whole hepatic lipid volume. Therefore, a single point or a few points on single slice calculation by ^{1}H-MRS or MRI-based PDFF methods would be difficult to use in the longitudinal comparison due to uneven lipid distribution and alteration of lipid distribution during the follow-up period.

In the present study, we aimed to establish an alternative ideal method for absolute quantification of whole hepatic lipid volume and hepatic lipid mapping by multi-slice and multi-point calculation of MR images. Furthermore, to validate this new method, we compared the accuracies of MRI and ^{1}H-MRS in diagnosing steatosis based on liver biopsy results.

Materials and Methods

Study design and population

In this retrospective study, clinical data of subjects included in our previous prospective studies on hepatic insulin sensitivity and hepatic steatosis conducted between November 2014 and January 2019 at the Toho University Hospital were used. Fifty-two patients aged 20-70 years who were diagnosed with hepatic steatosis by US and agreed to undergo liver biopsies were included in this study. Patients with liver diseases such as hepatitis B or C, autoimmune hepatitis, drug-induced hepatitis, and alcoholic hepatitis, or any other diseases except type 2 diabetes mellitus, hypertension, or dyslipidemia were excluded. Eight healthy subjects without hepatic steatosis were also included as controls. The interval among MRI, biopsy, and laboratory test was three days in this study. All measurements were performed after an overnight fast.

The study protocol was approved by the Ethics Committee of Toho University Omori Medical Center (No. M18155) and was conducted according to the Declaration of Helsinki and the current legal regulations in Japan. Written informed consent was obtained from all patients in previous prospective studies, and patients had the right to opt out of this study.

^{1}H-MRS

^{1}H-MRS was performed after an overnight fast as described previously.[21] Briefly, intrahepatic lipid content was measured at the liver segment #6 by ^{1}H-MRS using a whole-body 1.5-T unit (Magnetom Avanto, Siemens Healthcare, Tokyo, Japan) with a whole body coil. A single voxel (2×2×2 cm^3) was manually placed on the liver,

avoiding liver edges, visible blood vessels, and bile ducts. Shimming and tuning were performed manually. The spectra were obtained by point-resolve spectroscopy sequences (repetition time ms/echo time ms, 4000/30; acquisition time, 8 s). MR spectral raw data were processed to calculate intrahepatic lipid content using the LC model software (version 6.3-1J, Stephen Provencher, Oakville, ONT, Canada). Intrahepatic lipid content was quantified using methylene signal intensity (S-fat) at 1.3 ppm and H_2O at approximately 4.7 ppm as the internal reference.[12, 14] Intrahepatic lipid content was calculated as a percentage of S-fat using the following formula: {S-fat/(H_2O＋S-fat)}×100.[22] ^{1}H-MRS measurement was performed by three experienced technicians blinded to the identity of the subjects and clinical information.

Whole hepatic lipid volume measurement with MRI

MRI was performed using the Magnetom Avanto 1.5 T MRI system (Siemens Healthcare, Tokyo, Japan) by experienced technicians blinded to the identity of the subjects and clinical information. Hepatic steatosis was evaluated by identifying the differences in resonant frequencies between the protons in fat and those in water.[23] The MRI was performed according to the modified Dixon method, as described previously.[24-26] Briefly, all patients were placed in the supine position and were carefully instructed to be consistent in their breath holds. The sequence, which was performed through the liver, was a transverse breath-hold with the following parameters: repetition time ms/echo time ms, 6.98/2.4 (opposed phase), 6.98/4.8 (in phase); flip angle, 13.0°; matrix, 320/156; number of sections, around 52; and acquisition time, less than 26 s. Number of sections and acquisition time were decided depending on the patients' body size. This method could provide water-only and fat-only images separately. Initially, to

obtain liver-specific images, water-only images were used to separate the liver from all the whole abdomen slices; thereafter, the separated area could be traced in the same slices with fat-only images corresponding to water-only images using specific analysis software (Virtual Place ver. 3.6, AZE, Tokyo). These processes were performed semi-automatically and confirmed by four experienced technicians blinded to the identity of the subjects and clinical information.

Subsequently, these images were translated to digital imaging and communications in medicine data. Using a dedicated software (Analyze Software, Mayo Clinic, Rochester, MI, USA), whole liver images were evaluated based on the composition of all voxels. Information on not only the total number of voxels but also voxel width, length, and height per liver were obtained from the digital imaging and communications in medicine data. The separated hepatic water and fat images were combined using the formula Fat / (Water + Fat), as previously described[7]; thus, the signal fat fraction could be assessed and the ratio of hepatic lipid accumulation could be calculated for all slices. The signal of fat fraction per voxel was represented as the signal intensity within a range of 0%–100%, and each voxel color was defined by the ratio of hepatic lipid accumulation as follows: hepatic lipid ratio <5%, blue; ≥5 and <20%, green; ≥20 and <30%, yellow; ≥30 and <40%, orange; and ≥40%, red (Fig. S1). Hepatic lipid accumulation expressed by color gradation range was identified from all slices of the liver images with a full dynamic range (0%–100%). We first multiplied the intensity range of 0%–100% by the voxel numbers of each intensity. The total signal fat fraction was obtained by multiplying the sum of all voxel intensities by the voxel numbers (A) (Fig. S2). If all voxels consisted of 100% lipid, total hepatic lipid intensity was

calculated as 100×voxel number (B). The ratio of total signal fat fraction in the liver as the whole hepatic lipid ratio was obtained using the following formula: (A/B)×100 (%). Total liver volume was calculated using the following formula: total liver volume = width (X)×length (Y)×height (Z)×total voxel number (X, Y, Z, and voxel number were determined during the acquisition of MR images). Finally, whole hepatic lipid volume was calculated by multiplying the total liver volume by whole hepatic lipid ratio. In this study, the whole hepatic lipid volume was corrected by body surface area.

Liver biopsy

Fifty-two patients diagnosed as having hepatic steatosis by US agreed to undergo liver biopsy. Liver biopsy was not performed in eight subjects without hepatic steatosis. US-guided liver needle biopsies were performed at unit V based on the Couinaud classification using a 16-gauge liver biopsy needle (Core IITM semiautomatic biopsy instrument; InterV Clinical Products, Dartmouth, MA). Liver biopsy specimen was fixed in 10% formalin and used for histopathologic examination. Samples were embedded in paraffin, sectioned, and stained with hematoxylin and eosin along with azan. Histological characteristics, NAFLD activity score, and fibrosis were evaluated using standard histological criteria[27] by an experienced pathologist blinded to the identity of the subjects and clinical information. NAFLD activity score was determined based on histopathological features of steatosis (0–3), lobular inflammation (0–3), and hepatocellular ballooning (0–2). Steatosis was scored as follows: <5%=0, 5–33%=1, >33–66%=2, and >66%=3. For lobular inflammation, the scoring was as follows: no foci=0, <2 foci=1, 2–4 foci=2, and >4 foci=3. Hepatocellular ballooning was scored as follows: none=0, few=1, and many=2. Scores of each feature were summed, and a total

score of 0–2 indicated no steatohepatitis, 3–4 possible/borderline steatohepatitis, and 5–8 definite steatohepatitis. Moreover, fibrosis stage was scored as follows: none=0, mild at zone 3=1A, moderate at zone 3=1B, portal/periportal=1C, zone 3 and periportal=2, bridging=3, and cirrhosis=4.

Laboratory tests

Hemoglobin A1c, fasting plasma glucose, and alanine transaminase were measured at the central laboratory of the hospital or at an outsourced private laboratory (SRL Laboratory, Tokyo, Japan).

Statistical analysis

All data are expressed as mean ± standard deviation (SD), unless otherwise indicated. The accuracy of MRI and ^{1}H-MRS in diagnosing hepatic steatosis stages ≥1, ≥2, and ≥3 (classified according to steatosis score using standard histological criteria) was compared using receiver operating characteristic (ROC) analysis. The area under the ROC curve (AUROC) and performance parameters (i.e., sensitivity, specificity, positive predictive value, and negative predictive value) were evaluated using SAS software (version 9.4, SAS Institute, Cary, NC), and the optimal cutoff value of AUROC was identified. The optimal cutoff value of each modality was estimated using the Youden index.[28] Moreover, Delong test was performed to compare the AUROCs of MRI and ^{1}H-MRS in diagnosing hepatic steatosis.[29] Simple linear regression analysis was performed to assess the association between two methods regarding continuous variables, and the Kruskal-Wallis test was used for categorical variables using the

program PRISM Version 7 (GraphPad Software, La Jolla, CA). P values <0.05 were considered statistically significant.

Results

Clinical characteristics of the study subjects

Clinical characteristics of the study subjects are shown in Table 1. Sixty subjects including 52 patients with hepatic steatosis and 8 healthy subjects without hepatic steatosis, as assessed by US, were evaluated in this study. The cohort included 41 men and 19 women. The patients with hepatic steatosis were middle aged and obese (body mass index 29.8 ± 5.3 kg/m^2, mean ± SD), and the prevalence of type 2 diabetes mellitus was high (71.2%). Their average intrahepatic lipid content assessed using ^{1}H-MRS was 20.4 ± 10.1%, and the average ratio of whole hepatic lipid accumulation assessed by our new MRI analysis method was 19.7 ± 8.6%. Moreover, the NAFLD activity scores of patients with hepatic steatosis who agreed to undergo liver biopsy were as follows: 0 (n=5), 1 (n=6), 2 (n=12), 3 (n=14), 4 (n=10), 5 (n=3), and 6 (n=2). Finally, five nonalchoholic steatohepatitis patients having NAFLD activity score of 5 or 6 were included in this study. Fibrosis scores were ≤2 in 90% of patients who underwent liver biopsies.

Diagnostic accuracy of the new MRI analysis method

To compare the diagnostic accuracy of the new MRI analysis method with that of ^{1}H-MRS, the ROC curve and potential cutoff values for the diagnosis of hepatic steatosis were calculated in the subjects who underwent a liver biopsy. The ROC curves for differentiating between MRI and ^{1}H-MRS based on hepatic steatosis score 0 and 1–3, 0–1 and 2–3, and 0–2 and 3 are shown in Fig. 1A to Fig. 1C, respectively. The AUROC for diagnosing hepatic steatosis stages ≥1, ≥2, and ≥3 using MRI and ^{1}H-MRS were 0.860 (95% confidence interval [CI]: 0.700–1.000) and 0.975 (95% CI: 0.933–1.000);

0.936 (95% CI: 0.873–1.000) and 0.929 (95% CI: 0.860–0.998); and 0.951 (95% CI: 0.890–1.000) and 0.969 (95% CI: 0.928–1.000), respectively (Table 2). The cutoff value and sensitivity, specificity, positive predictive value, and negative predictive value for each hepatic steatosis score are also shown in Table 2. These results indicate that the diagnostic accuracy was comparable between MRI and ^{1}H-MRS.

Hepatic lipid accumulation correlation and differences between the new MRI analysis and ^{1}H-MRS methods

Linear regression analysis was performed for hepatic lipid accumulation evaluation. Initially, we compared our newly developed lipid accumulation assessment with histopathological assessment. The ratio of lipid accumulation in the whole liver assessed by the new MRI analysis method was significantly associated with the steatosis score of the NAFLD activity score in 52 patients who had liver biopsy (Fig. 2A). On the other hand, the other NAFLD activity scores such as inflammation or ballooning scores or fibrosis stages showed no association with the ratio of lipid accumulation in the whole liver assessed by the new MRI analysis method (Fig. S3). A significant correlation between the ratio of lipid content in whole liver measured by the new MRI analysis method and the intrahepatic lipid content measured by ^{1}H-MRS was also noted (Fig. 2B). The coefficient of determination was 0.883 (p<0.001), indicating a strong linear relationship. In addition, the whole hepatic lipid volume calculated by the new MRI analysis method significantly correlated with intrahepatic lipid content measured by ^{1}H-MRS (Fig. 2C). The coefficient of determination was 0.782 (p<0.001).

Data on hepatic lipid accumulation as assessed by the two methods were closely associated; however, some inconsistency between the methods was observed (Fig. 2B, C). Fig. 3A, C, E, G shows the graduated color mapping expressing hepatic lipid accumulation intensity based on the new MRI analysis method. In cases without steatosis or homogeneous lipid accumulation (Fig. 3A, C), the calculated lipid accumulation levels were quite similar between the methods (Fig. 3B, D, respectively). However, some cases had heterogeneous lipid accumulation (Fig. 3E, G), and the lipid accumulation levels were significantly different (around two-fold) between the methods (Fig. 3F, H). Specifically, intrahepatic lipid content measured by ^{1}H-MRS was 44.3%, whereas the whole hepatic lipid ratio measured by the new MRI analysis method was 27.2% (Fig. 3E, F). Moreover, intrahepatic lipid content measured by ^{1}H-MRS was 6.9%, whereas whole hepatic lipid ratio measured by the new MRI analysis method was 18.3% (Fig. 3G, H).

Discussion

In this study, we developed a new analysis method for absolute quantification of whole hepatic lipid accumulation using multi-slice and multi-point MRI. Whole hepatic lipid ratio assessed by the newly developed MRI analysis method showed a significantly strong association with intrahepatic lipid content assessed by ^{1}H-MRS. ROC curve analysis demonstrated that this method is comparable to the ^{1}H-MRS method for hepatic steatosis assessment. Furthermore, this MRI analysis method could produce graduated color mapping showing hepatic lipid accumulation intensity and demonstrate the existence of heterogeneous lipid accumulation that may cause over- or underestimation of hepatic steatosis. The advantage of our multi-slice and multi-point MRI analysis method is its capability to absolutely and objectively quantify whole hepatic lipid volume, in addition to whole hepatic lipid ratio, which in turn results in an accurate and reproducible longitudinal evaluation of hepatic steatosis.

According to previous studies, both MRI and MRS are non-invasive, repeatable imaging methods for hepatic lipid accumulation evaluation.[9, 11-19, 30, 31] In the present study, AUROC for distinguishing steatosis score >1 of whole hepatic lipid ratio by MRI tended to be lower than that of intrahepatic lipid content measured by ^{1}H-MRS although there was no significant difference. Regarding this, liver biopsy was performed in the right lobe segment V, and in ^{1}H-MRS measurement, region of interest was also set at the right lobe. Previously, it was reported that hepatic lipid accumulation was tended to be more observed in the right lobe than the left lobe.[32, 33] Thus, in the condition of hepatic lipid accumulation less than 33%, that is steatosis score 1, whole hepatic lipid ratio that includes the data of left lobe might be tended to be lower than the data that

assessed only right lobe, leading to the lower sensitivity in the new MRI analysis method than ^{1}H-MRS method (Fig. 1A). On the other hand, in the condition of hepatic lipid accumulation more than 33% or higher, lipid accumulation might be largely observed including left lobe because lipid might distribute throughout the liver, leading to the similar sensitivity and specificity between the new MRI analysis and ^{1}H-MRS method (Fig. 1B and C). However, ^{1}H-MRS is associated with sampling error because it can only assess the signal of a small, single voxel. Some researchers mentioned that ^{1}H-MRS has methodical limitation attributed to fat distribution variation among different regions of the liver,[14, 34] and they suggested the importance of whole hepatic lipid accumulation assessment.[14] Moreover, some studies showed a weak association between ^{1}H-MRS and histological evaluation of hepatic lipid accumulation.[12, 16, 19] Thus, evaluation of a small part of the liver is not enough, especially because the lipid distribution in the liver varies (i.e., diffuse, focal, perilesional, periportal-perivascular, subcapsular, lobular, and multinodular).[34-38] In addition, some intrahepatic lipid content measured by ^{1}H-MRS was overestimated or underestimated because of fat distribution in our NAFLD patients (Fig. 3). Interestingly, this phenomenon also occurred in eight healthy subjects. In fact, intrahepatic lipid content measured by ^{1}H-MRS was 4.20% (maximum) and 0.25% (minimum), while the whole hepatic lipid ratio measured by the new MRI analysis method was 4.89% (maximum) and 4.15% (minimum). Although the two-point Dixion method and fat maps based on NAFLD activity score were introduced as a useful method to assess hepatic lipid content,[39] the advantage of our method is that it could provide the actual lipid volume of the whole liver and the graduated color mapping showing lipid accumulation throughout the liver. Furthermore, it could evaluate the whole liver volume by calculating the total voxels' volume and the whole

hepatic lean volume by subtracting the whole hepatic lipid volume from the whole liver volume. Therefore, once the patients undergo MRI examination, our method can provide data of the whole hepatic lipid ratio, liver volume, hepatic lipid volume, and hepatic lean volume at once. This is the first such method described and can potentially be widely applied not only for steatosis assessment but also for hepatic parenchymal assessment in liver failure, atrophy, transplantation, or regeneration. Recently, MRI-based PDFF method is gaining popularity[8, 10, 40]; however, this method provides only the fat ratio data but not absolute lipid volume or parenchymal volume data. Because liver failure, atrophy, transplantation, and regeneration are all related to advanced NAFLD or nonalcoholic steatohepatitis,[41-43] our new multi-slice and multi-point MRI analysis method would have an advantage over other methods in terms of volume assessment.

The need for a specific software for both MRI and MRS protocols may be a challenge in terms of availability. However, the protocol for MRI with Dixon in-phase/out-of phase is more common and feasible than that for ^{1}H-MRS, which needs a special coil and setting. Another advantage of the new multi-slice and multi-point MRI analysis method is that whole lipid accumulation in the liver could be calculated after examining MR images and obtaining Dixon raw data; thus, any hospital could send Dixon raw data files to available facilities for calculation. By contrast, the region of interest for ^{1}H-MRS should be set and signals must be obtained while the patients undergo MRI, and when recalculation is necessary, patients need to undergo MRI again for the ^{1}H-MRS method.

In this study, we also compared whole lipid accumulation evaluated by our MRI analysis method with hepatic lipid accumulation evaluated by histopathologic

assessment. Regarding the diagnosis of NASH, liver biopsy is the established standard method; however, it has some clinical drawbacks because it is invasive and associated with sampling error and variability.[44, 45] In addition, the liver biopsy is very expensive. Although liver biopsy itself costs 16,000 yen, all patients who undertake liver biopsy must be hospitalized for three days for the safety issue and hospitalization costs about 160,000 yen. In contrast, the new MRI analysis method costs only 20,000 yen that is the same amount as routine MRI cost. Hence, liver biopsy is not suitable for common clinical use in hepatic steatosis assessment. In addition, histopathological assessment can evaluate only a small part of a hepatic specimen (approximately 10–15 mg); however, it appears that hepatic histological condition differs depending on the region selected for sampling. In the past study, sampling variability of liver biopsy was assessed in patients with NAFLD.[4] As results, a significant difference (>20 % of hepatocytes) was found about steatosis between paired biopsy specimens in 18% of patients. In addition, it was mentioned that sampling error was considered partly as an intraobserver variability but largely as an influence of the heterogeneity of the distribution of lipid accumulation. In contrast, the new multi-slice and multi-point MRI analysis method is easy to perform and could avoid sampling errors.

For longitudinal observation, ^{1}H-MRS and liver biopsy are not suitable for repeated assessments because it is difficult to maintain the same voxel region or needle biopsy area through multiple follow-ups. In addition, even if the sampling region is set at the same place, sampling conditions may vary during the follow-up period. Thus, reproducibility of both methods is uncertain. Recently, it was reported that MRI-based PDFF method could accurately classify steatosis,[5, 6] furthermore, nine ROIs placed in

each hepatic segment has been used to reduce the variation in MRI-PDFF method quite recently.[33] Therefore, it has become more accurate than before. However, its reproducibility is still uncertain due to the measurement using a limited number of regions of interest, and because it provides the fat ratio data it may have some limitations for the use in longitudinal observations. Quite recently, it was also reported that MRI-based PDFF method was suboptimal in identification of patients with NAFLD activity score >4 or advanced fibrosis.[46] By contrast, the new multi-slice and multi-point MRI analysis method has no such limitations, is reproducible, and could be performed repeatedly; therefore, reduction or increase in hepatic lipid content could be accurately assessed and compared. In near future, the present new MRI analysis method is desired to be compared directly with the current MRI-PDFF method from the various angles.

Although we demonstrated that the new multi-slice and multi-point MRI analysis method is ideal for the accurate longitudinal assessment of hepatic steatosis, our study has some potential limitations. First, processing of whole liver images in a single patient with color mapping and whole hepatic lipid volume calculation takes approximately 30 min. While image processing is performed semi-automatically, objectively, and accurately using specific software programs, further improvement is necessary for general clinical use. In addition, artificial intelligence use is rapidly spreading and may largely assist image processing and calculation in the near future. Second, iron may influence the evaluation of steatosis and is thus a potential limiting factor for MR; however, this could not be completely eliminated as hepatic iron is common in patients with chronic liver disease.[13, 47] Finally, our study included a small number of Japanese patients, and most patients in this study had a low fibrosis stage. Hence, our findings

need to be tested in a larger number of patients of different ethnicities and in patients with progressed fatty liver disease.

In conclusion, this is the first study that evaluated whole hepatic lipid accumulation using multi-slice and multi-point MRI and compared the accuracy of this new method to that of ^{1}H-MRS in hepatic steatosis assessment. Our results demonstrated that whole hepatic lipid ratio assessed by the new multi-slice and multi-point MRI analysis method is comparable to intrahepatic lipid content measured by ^{1}H-MRS. In addition, not only whole hepatic lipid ratio but also whole liver volume and whole hepatic lipid volume could be evaluated by the new multi-slice and multi-point MRI analysis method. Subsequently, whole hepatic lean volume that is suitable for hepatic parenchymal assessment can be calculated with this method. Furthermore, graduated color mapping of the liver, which could show variation in hepatic lipid accumulation, is possible. Therefore, the multi-slice and multi-point MRI analysis is reliable and useful for the longitudinal observation of hepatic steatosis and the evaluation of treatment efficacy.

Acknowledgment

We thank the participants in this study. We are grateful to Hirokazu Yamada for his excellent assistance in the statistical analyses. We also thank Motoharu Ohtsu, Ichikawa Kouji, and Hisanobu Harada for their excellent technical assistance. We would like to thank Editage (www.editage.jp) for English language editing. This research was supported by JSPS KAKENHI (Grant Numbers 26702032 and JP17H02180).

Conflict of Interest and Source of Funding

N. Kumashiro received research funds from Boehringer Ingelheim Pharmaceuticals, Inc., and received lecture fees from Novo Nordisk Inc., Takeda Pharmaceutical Company Limited, Ono Pharmaceutical Co., Ltd., and Sanofi-Aventis Deutschland GmbH. T. Hirose received research funds from AstraZeneca, Boehringer Ingelheim Pharmaceuticals, Inc., Ono Pharmaceutical Co., Ltd., Novo Nordisk Inc., Sanofi-Aventis Deutschland GmbH, Daiichi-Sankyo Co., Ltd., Eli Lilly Japan K.K., Takeda Pharmaceutical Company Limited, Mitsubishi Tanabe Pharma Corporation, Dainippon Sumitomo Pharma Co., Ltd., and Kissei Pharmaceutical Co., Ltd., and received lecture fee from Sanofi-Aventis Deutschland GmbH, Eli Lilly Japan K.K., Novo Nordisk Inc., Takeda Pharmaceutical Company Limited, Daiichi-Sankyo Co., Ltd., Mitsubishi Tanabe Pharma Corporation, Merck & Co., Inc., Dainippon Sumitomo Pharma Co., Ltd., Novartis Pharma K.K., Kissei Pharmaceutical Co., Ltd., Boehringer Ingelheim Pharmaceuticals, Inc., Ono Pharmaceutical Co., Ltd., and AstraZeneca. All funding agencies had no role in the study design, data collection and analysis, decision to publish, or preparation of the manuscript. Other authors have nothing to disclose. This research was supported by JSPS KAKENHI (Grant Numbers 26702032 and JP17H02180).

References

1 Younossi ZM, Koenig AB, Abdelatif D, *et al.* Global epidemiology of nonalcoholic fatty liver disease-Meta-analytic assessment of prevalence, incidence, and outcomes. *Hepatology*. 2016; 64: 73-84.

2 Byrne CD, Targher G. NAFLD: a multisystem disease. *J Hepatol*. 2015; 62: S47-64.

3 Stinton LM, Loomba R. Recommendations for liver biopsy evaluation in non-alcoholic fatty liver disease. *Minerva Gastroenterol Dietol*. 2014; 60: 5-13.

4 Ratziu V, Charlotte F, Heurtier A, *et al.* Sampling variability of liver biopsy in nonalcoholic fatty liver disease. *Gastroenterology*. 2005; 128: 1898-1906.

5 Imajo K, Kessoku T, Honda Y, *et al.* Magnetic Resonance Imaging More Accurately Classifies Steatosis and Fibrosis in Patients With Nonalcoholic Fatty Liver Disease Than Transient Elastography. *Gastroenterology*. 2016; 150: 626-637 e627.

6 Park CC, Nguyen P, Hernandez C, *et al.* Magnetic Resonance Elastography vs Transient Elastography in Detection of Fibrosis and Noninvasive Measurement of Steatosis in Patients With Biopsy-Proven Nonalcoholic Fatty Liver Disease. *Gastroenterology*. 2017; 152: 598-607 e592.

7 Reeder SB, Cruite I, Hamilton G, *et al.* Quantitative assessment of liver fat with magnetic resonance imaging and spectroscopy. *J Magn Reson Imaging*. 2011; 34: 729-749.

8 Idilman IS, Aniktar H, Idilman R, *et al.* Hepatic steatosis: quantification by proton density fat fraction with MR imaging versus liver biopsy. *Radiology*. 2013; 267: 767-775.

9 Permutt Z, Le TA, Peterson MR, *et al.* Correlation between liver histology and novel magnetic resonance imaging in adult patients with non-alcoholic fatty liver disease - MRI accurately quantifies hepatic steatosis in NAFLD. *Aliment Pharmacol Ther*. 2012; 36: 22-29.

10 Tang A, Desai A, Hamilton G, *et al.* Accuracy of MR imaging-estimated proton density fat fraction for classification of dichotomized histologic steatosis grades in nonalcoholic fatty liver disease. *Radiology*. 2015; 274: 416-425.

11 Fishbein M, Castro F, Cheruku S, *et al.* Hepatic MRI for fat quantitation: its

relationship to fat morphology, diagnosis, and ultrasound. *J Clin Gastroenterol*. 2005; 39: 619-625.

12 Lee SS, Park SH, Kim HJ, *et al.* Non-invasive assessment of hepatic steatosis: prospective comparison of the accuracy of imaging examinations. *J Hepatol*. 2010; 52: 579-585.

13 McPherson S, Jonsson JR, Cowin GJ, *et al.* Magnetic resonance imaging and spectroscopy accurately estimate the severity of steatosis provided the stage of fibrosis is considered. *J Hepatol*. 2009; 51: 389-397.

14 van Werven JR, Marsman HA, Nederveen AJ, *et al.* Assessment of hepatic steatosis in patients undergoing liver resection: comparison of US, CT, T1-weighted dual-echo MR imaging, and point-resolved 1H MR spectroscopy. *Radiology*. 2010; 256: 159-168.

15 Szczepaniak LS, Nurenberg P, Leonard D, *et al.* Magnetic resonance spectroscopy to measure hepatic triglyceride content: prevalence of hepatic steatosis in the general population. *Am J Physiol Endocrinol Metab*. 2005; 288: E462-468.

16 Longo R, Pollesello P, Ricci C, *et al.* Proton MR spectroscopy in quantitative in vivo determination of fat content in human liver steatosis. *J Magn Reson Imaging*. 1995; 5: 281-285.

17 Longo R, Ricci C, Masutti F, *et al.* Fatty infiltration of the liver. Quantification by 1H localized magnetic resonance spectroscopy and comparison with computed tomography. *Invest Radiol*. 1993; 28: 297-302.

18 Szczepaniak LS, Babcock EE, Schick F, *et al.* Measurement of intracellular triglyceride stores by H spectroscopy: validation in vivo. *Am J Physiol*. 1999; 276: E977-989.

19 Thomsen C, Becker U, Winkler K, *et al.* Quantification of liver fat using magnetic resonance spectroscopy. *Magn Reson Imaging*. 1994; 12: 487-495.

20 Cowin GJ, Jonsson JR, Bauer JD, *et al.* Magnetic resonance imaging and spectroscopy for monitoring liver steatosis. *J Magn Reson Imaging*. 2008; 28: 937-945.

21 Shigiyama F, Kumashiro N, Furukawa Y, *et al.* Characteristics of hepatic insulin-sensitive nonalcoholic fatty liver disease. *Hepatol Commun*. 2017; 1:

634-647.

22 Ryysy L, Hakkinen AM, Goto T, *et al.* Hepatic fat content and insulin action on free fatty acids and glucose metabolism rather than insulin absorption are associated with insulin requirements during insulin therapy in type 2 diabetic patients. *Diabetes*. 2000; 49: 749-758.

23 Mazhar SM, Shiehmorteza M, Sirlin CB. Noninvasive assessment of hepatic steatosis. *Clin Gastroenterol Hepatol*. 2009; 7: 135-140.

24 Dixon WT. Simple proton spectroscopic imaging. *Radiology*. 1984; 153: 189-194.

25 Hussain HK, Chenevert TL, Londy FJ, *et al.* Hepatic fat fraction: MR imaging for quantitative measurement and display--early experience. *Radiology*. 2005; 237: 1048-1055.

26 Guiu B, Petit JM, Loffroy R, *et al.* Quantification of liver fat content: comparison of triple-echo chemical shift gradient-echo imaging and in vivo proton MR spectroscopy. *Radiology*. 2009; 250: 95-102.

27 Kleiner DE, Brunt EM, Van Natta M, *et al.* Design and validation of a histological scoring system for nonalcoholic fatty liver disease. *Hepatology*. 2005; 41: 1313-1321.

28 Youden WJ. Index for rating diagnostic tests. *Cancer*. 1950; 3: 32-35.

29 DeLong ER, DeLong DM, Clarke-Pearson DL. Comparing the areas under two or more correlated receiver operating characteristic curves: a nonparametric approach. *Biometrics*. 1988; 44: 837-845.

30 Kim H, Taksali SE, Dufour S, *et al.* Comparative MR study of hepatic fat quantification using single-voxel proton spectroscopy, two-point dixon and three-point IDEAL. *Magn Reson Med*. 2008; 59: 521-527.

31 Meisamy S, Hines CD, Hamilton G, *et al.* Quantification of hepatic steatosis with T1-independent, T2-corrected MR imaging with spectral modeling of fat: blinded comparison with MR spectroscopy. *Radiology*. 2011; 258: 767-775.

32 Hua B, Hakkarainen A, Zhou Y, *et al.* Fat accumulates preferentially in the right rather than the left liver lobe in non-diabetic subjects. *Dig Liver Dis*. 2018; 50: 168-174.

33 Hong CW, Wolfson T, Sy EZ, *et al.* Optimization of region-of-interest sampling

strategies for hepatic MRI proton density fat fraction quantification. *J Magn Reson Imaging*. 2018; 47: 988-994.

34 Idilman IS, Ozdeniz I, Karcaaltincaba M. Hepatic Steatosis: Etiology, Patterns, and Quantification. *Semin Ultrasound CT MR*. 2016; 37: 501-510.

35 Karcaaltincaba M, Akhan O. Imaging of hepatic steatosis and fatty sparing. *Eur J Radiol*. 2007; 61: 33-43.

36 Vilgrain V, Ronot M, Abdel-Rehim M, *et al.* Hepatic steatosis: a major trap in liver imaging. *Diagn Interv Imaging*. 2013; 94: 713-727.

37 Ozcan HN, Oguz B, Haliloglu M, *et al.* Imaging patterns of fatty liver in pediatric patients. *Diagn Interv Radiol*. 2015; 21: 355-360.

38 Dioguardi Burgio M, Bruno O, Agnello F, *et al.* The cheating liver: imaging of focal steatosis and fatty sparing. *Expert Rev Gastroenterol Hepatol*. 2016; 10: 671-678.

39 Hayashi T, Saitoh S, Takahashi J, *et al.* Hepatic fat quantification using the two-point Dixon method and fat color maps based on non-alcoholic fatty liver disease activity score. *Hepatol Res*. 2017; 47: 455-464.

40 Caussy C, Reeder SB, Sirlin CB, *et al.* Noninvasive, Quantitative Assessment of Liver Fat by MRI-PDFF as an Endpoint in NASH Trials. *Hepatology*. 2018; 68: 763-772.

41 Liu A, Galoosian A, Kaswala D, *et al.* Nonalcoholic Fatty Liver Disease: Epidemiology, Liver Transplantation Trends and Outcomes, and Risk of Recurrent Disease in the Graft. *J Clin Transl Hepatol*. 2018; 6: 420-424.

42 Mao SA, Glorioso JM, Nyberg SL. Liver regeneration. *Transl Res*. 2014; 163: 352-362.

43 Wong RJ, Aguilar M, Cheung R, *et al.* Nonalcoholic steatohepatitis is the second leading etiology of liver disease among adults awaiting liver transplantation in the United States. *Gastroenterology*. 2015; 148: 547-555.

44 Regev A, Berho M, Jeffers LJ, *et al.* Sampling error and intraobserver variation in liver biopsy in patients with chronic HCV infection. *Am J Gastroenterol*. 2002; 97: 2614-2618.

45 Bedossa P, Dargere D, Paradis V. Sampling variability of liver fibrosis in chronic hepatitis C. *Hepatology*. 2003; 38: 1449-1457.

46 Wildman-Tobriner B, Middleton MM, Moylan CA, *et al*. Association Between Magnetic Resonance Imaging-Proton Density Fat Fraction and Liver Histology Features in Patients With Nonalcoholic Fatty Liver Disease or Nonalcoholic Steatohepatitis. *Gastroenterology*. 2018; 155: 1428-1435 e1422.

47 van der Jagt MF, Sweep FC, Waas ET, *et al*. Correlation of reversion-inducing cysteine-rich protein with kazal motifs (RECK) and extracellular matrix metalloproteinase inducer (EMMPRIN), with MMP-2, MMP-9, and survival in colorectal cancer. *Cancer Lett*. 2006; 237: 289-297.

Appendices

Figure S1 The system of the color-mapped lipid distribution

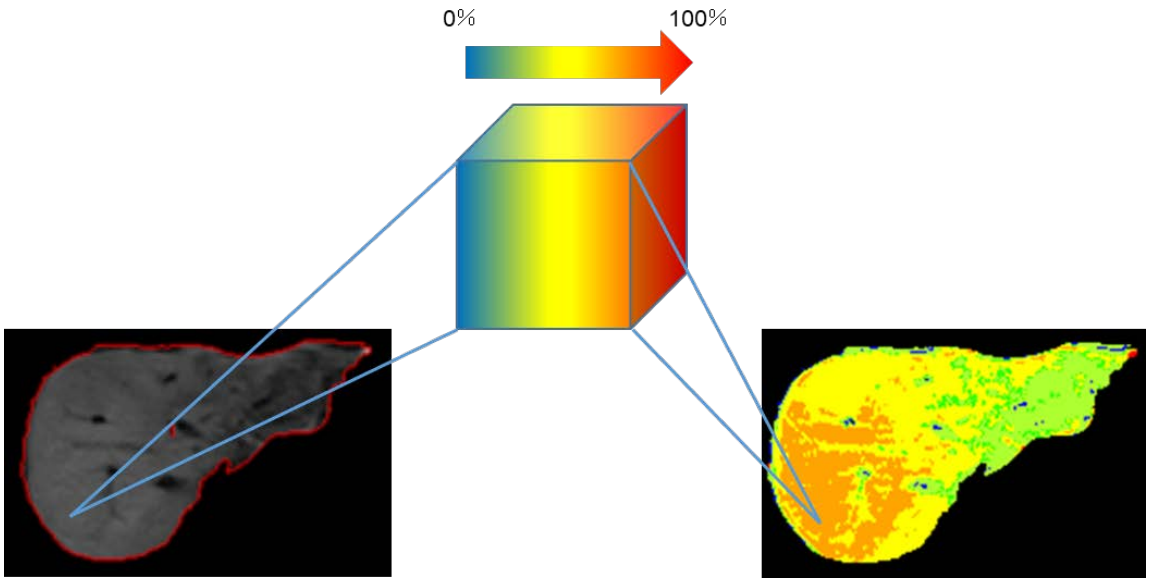

The separated hepatic water and fat images were combined by the formula Fat / (Water +Fat) using the dedicated software (Analyze Software, Mayo Clinic, Rochester, MI, USA) (left image). The signal of the fat fraction per voxel was represented as signal intensity within the range of 0%–100% (middle image), and the ratio of hepatic lipid accumulation was calculated. Each voxel color was classified by the ratio of hepatic lipid accumulation as follows: hepatic lipid ratio <5%, blue; ≥5 and <20%, green; ≥20 and <30%, yellow; ≥30 and <40%, orange; and ≥40%, red. Graduated color mapping image (right image).

Figure S2 Calculation system of the hepatic lipid content using multi-slice and multi-point magnetic resonance imaging

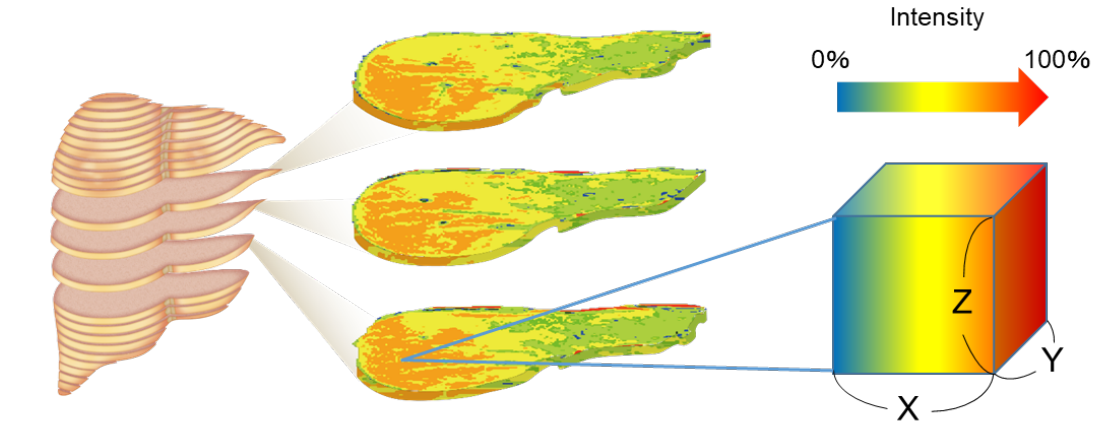

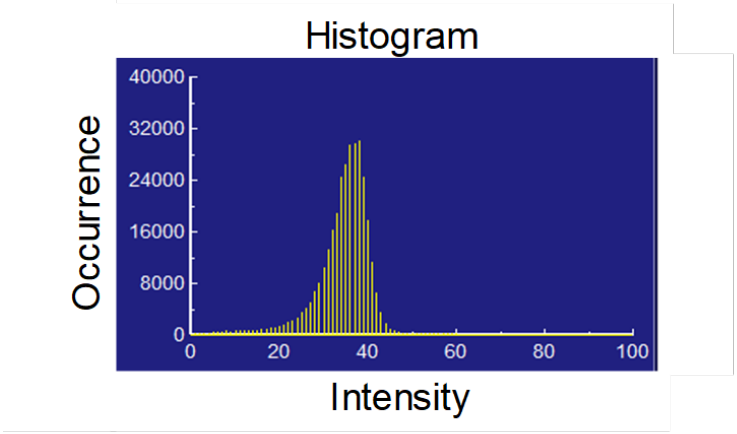

$$\text{Whole hepatic lipid ratio} = \frac{\sum_{n=0}^{100}\{Intensity(n) \times voxel\ number\}}{100 \times voxel\ number} \times 100$$

$$\text{Total liver volume} = X \times Y \times Z \times voxel\ number$$

$$\text{Whole hepatic lipid volume} = X \times Y \times Z \times voxel\ number \times \left[\frac{\sum_{n=0}^{100}\{Intensity(n) \times voxel\ number\}}{100 \times voxel\ number}\right]$$

The formula for calculation of whole hepatic lipid ratio, total liver volume, and whole hepatic lipid volume used in the new multi-slice and multi-point MRI analysis method. The width (X), length (Y), and height (Z) of voxel and the voxel number were determined during the acquisition of MR images. Lipid intensity of each voxel was calculated using the dedicated software (Analyze Software, Mayo Clinic, Rochester, MI, USA).

Figure S3　Association between whole hepatic lipid ratio and various scores using liver biopsy

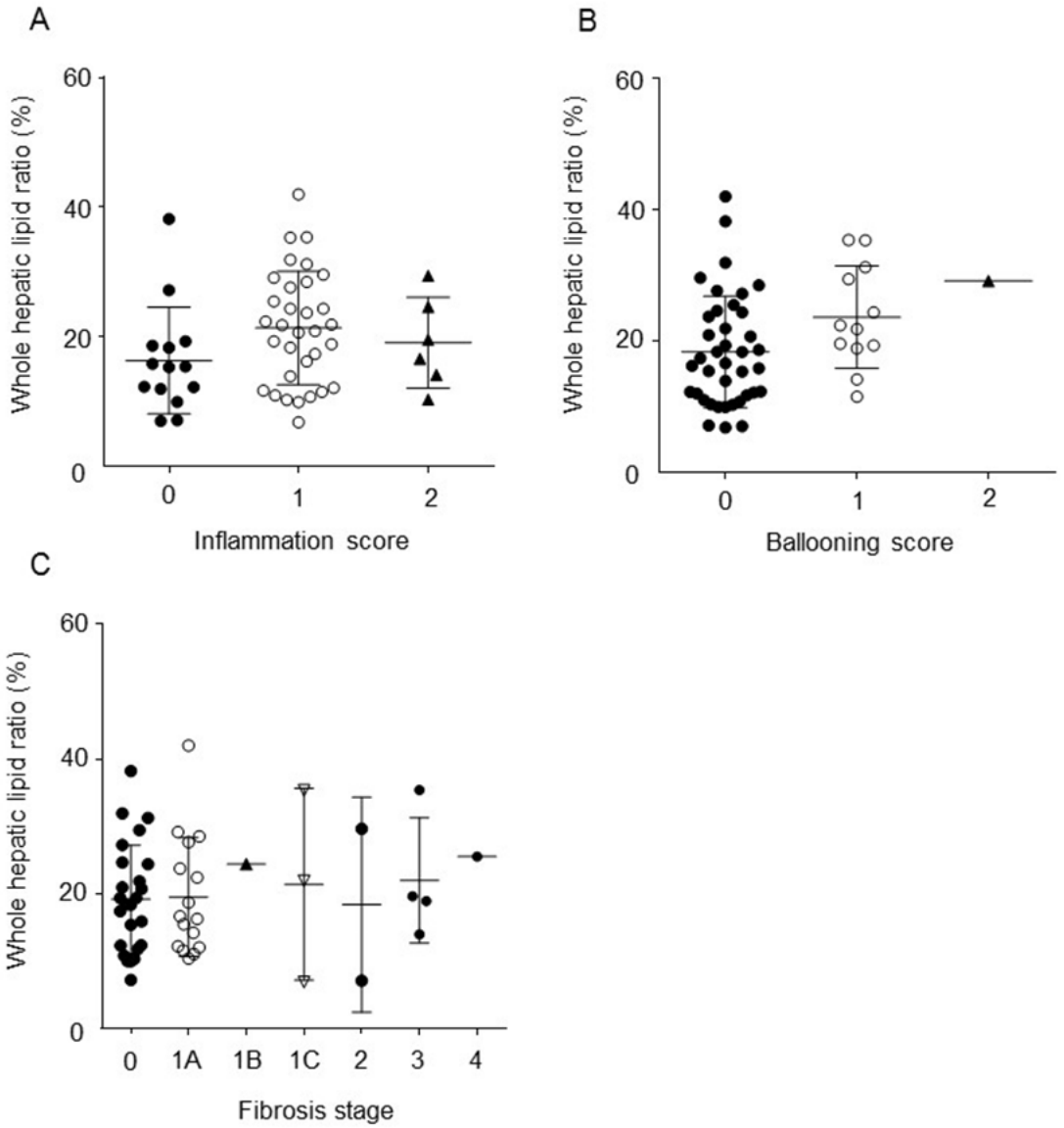

Distribution of the whole hepatic lipid ratio assessed by MRI and (A) the inflammation score of NAFLD activity score, (B) the ballooning score of NAFLD activity score, (C) fibrosis stage (n=52). (A) Statistical analysis was performed using Kruskal-Wallis test (p=0.15). No patient was scored as 3 for inflammation. (B, C) We couldn’t perform Kruskal-Wallis test because some of scores or stages included no patient or only one patient.

Figure Legends

Fig. 1. Diagnostic accuracy of the new MRI analysis method in assessing hepatic steatosis.

Diagnostic accuracy of the new MRI analysis and ^{1}H-MRS methods in assessing hepatic steatosis based on steatosis score of the NAFLD activity score in 52 patients who had liver biopsies. The area under the ROC curve (AUROC) for the performance of the new MRI analysis method or ^{1}H-MRS in distinguishing steatosis score 0 from scores ≥1 (A), 0-1 from ≥2 (B), and 0-2 from 3 (C) was identified. Statistical comparisons between the new MRI analysis method and ^{1}H-MRS were performed using Delong test. (A) p=0.12, (B) p=0.68, (C) p=0.50. ^{1}H-MRS, proton magnetic resonance spectroscopy; MRI, magnetic resonance imaging; NAFLD, nonalcoholic fatty liver disease; NAS, NAFLD activity score

Fig. 2. Association between whole hepatic lipid assessment and steatosis score by needle biopsy or intrahepatic lipid content by ^{1}H-MRS.

(A) Distribution of the whole hepatic lipid ratio assessed by MRI and the steatosis score of NAFLD activity score (n=52). Statistical analysis was performed using Kruskal-Wallis test ($p<0.001$). (B) Correlation between whole hepatic lipid ratio measured by MRI and the intrahepatic lipid content measured by ^{1}H-MRS (n=60). Simple linear regression analysis was performed ($p<0.001$). (C) Correlation between the whole hepatic lipid volume calculated by MRI and the intrahepatic lipid content calculated by ^{1}H-MRS (n=60). Simple linear regression analysis was performed ($p<0.001$). ^{1}H-MRS,

proton magnetic resonance spectroscopy; MRI, magnetic resonance imaging; NAFLD, nonalcoholic fatty liver disease

Fig. 3. Graduated color mapping of hepatic steatosis shows heterogeneous lipid accumulation and explains the different results between the methods.

(A, C, E, and G) Graduated color mapping expressing the intensity of hepatic lipid accumulation evaluated by MRI. A single voxel was put on liver segment #6 and used for the measurement in ^{1}H-MRS. (B, D, F, and H) Correlation between whole hepatic lipid ratio measured by MRI and intrahepatic lipid content measured by ^{1}H-MRS (n=60). Simple linear regression analysis was performed ($p<0.001$). The red dots in panel (B), (D), (F) and (H) show the data obtained from the patients in panel (A), (C), (E), and (G), respectively. ^{1}H-MRS, proton magnetic resonance spectroscopy; MRI, magnetic resonance imaging

Table 1. Characteristics of the study subjects

Characteristics	Steatosis (-) by US	Steatosis (+) by US
n	8	52
Age (years)	30.3+4.0	48.0 ± 12.2
Sex (male / female), n (%)	4 (50.0) / 4 (50.0)	37 (71.2) / 15 (28.8)
Body weight (kg)	57.0 ± 8.5	83.0 ± 16.7
Body mass index (kg/m^2)	20.6 ± 2.0	29.8 ± 5.3
Body surface area (m^2)	1.59 ± 0.15	1.87 ± 0.21
Diabetes / no diabetes, n (%)	0 (0.0) / 8 (100.0)	37(71.2) / 15 (28.8)
Alanine aminotransferase (IU/L)	14.3 ± 4.1	61.2 ± 28.3
Intrahepatic lipid (%)	1.4 ± 1.4	20.4 ± 10.1
Whole hepatic lipid ratio (%)	4.6 ± 0.3	19.7 ± 8.6
Whole hepatic lipid volume (cm^3/m^2)	31.9 ± 2.4	188.2 ± 107.3
Total NAFLD activity score, n (%)		
0		5 (9.6)
1		6 (11.5)
2		12 (23.1)
3		14 (26.9)
4		10 (19.2)
5		3 (5.8)
6		2 (3.8)
Steatosis, n (%)		
0 - <5%		5 (9.6)
1 - 5–33%		22 (42.3)
2 - 34–66%		16(30.8)
3 - >66%		9 (17.3)
Lobular inflammation, n (%)		
0 - none		14 (26.9)
1 - <2 foci		32 (61.5)
2 - 2–4 foci		6 (11.5)
3 - >4 foci		0 (0.0)
Hepatocellular ballooning, n (%)		

0 - none	39 (75.0)
1 - few	12 (23.1)
2 - many	1 (1.9)
Fibrosis score, n (%)	
0 - none	25 (48.1)
1A - mild at zone 3	16 (30.8)
1B - moderate at zone 3	1 (1.9)
1C - portal/periportal	3 (5.8)
2 - zone 3 and periportal	2 (3.8)
3 - bridging	4 (7.7)
4 - cirrhosis	1 (1.9)

Data are mean±SD. Liver biopsy was performed on 52 patients. Total NAFLD activity score was the sum of the scores of the following histopathological features: steatosis (0–3), lobular inflammation (0–3), and hepatocellular ballooning (0–2).

NAFLD, non-alcoholic fatty liver disease; US, ultrasonography

Table 2. Diagnostic accuracy of steatosis score of the NAFLD activity score

	Intrahepatic lipid content by ^{1}H-MRS	Whole hepatic lipid ratio by MRI
Steatosis score ≥ 1	(n=47) vs. score 0 (n=5)	
AUROC	0.975 [0.933, 1.000]	0.860 [0.700, 1.000]
AUROC *p* value	-	0.12
Cutoff value	9.6	18.4
Sensitivity	91.5 (43/47) [79.6, 97.6]	59.6 (28/47) [44.3, 73.6]
Specificity	100 (5/5) [47.8, 100]	100 (5/5) [47.8, 100]
PPV	100 (43/43) [91.8, 100]	100 (28/28) [87.7, 100]
NPV	55.6 (5/9) [21.2, 86.3]	20.8 (5/24) [7.1, 42.2]
Steatosis score ≥ 2	(n=25) vs. score 0–1 (n=27)	
AUROC	0.929 [0.860, 0.998]	0.936 [0.873, 1.000]
AUROC *p* value	-	0.68
Cut off value	19.5	18.4
Sensitivity	92.0 (23/25) [74.0, 99.0]	92.0 (23/25) [74.0, 99.0]
Specificity	85.2 (23/27) [66.3, 95.8]	81.5 (22/27) [61.9, 93.7]
PPV	85.2 (23/27) [66.3, 95.8]	82.1 (23/28) [63.1, 93.9]
NPV	92.0 (23/25) [74.0, 99.0]	91.7 (22/24) [73.0, 99.0]
Steatosis score ≥ 3	(n=9) vs. score 0–2 (n=43)	
AUROC	0.969 [0.928, 1.000]	0.951 [0.890, 1.000]
AUROC *p* value	-	0.50
Cutoff value	29.2	27.2
Sensitivity	100 (9/9) [66.4, 100]	88.9 (8/9) [51.8, 99.7]
Specificity	90.7 (39/43) [77.9, 97.4]	90.7 (39/43) [77.9, 97.4]
PPV	69.2 (9/13) [38.6, 90.9]	66.7 (8/12) [34.9, 90.1]
NPV	100 (39/39) [91.0, 100]	97.5 (39/40) [86.8, 99.9]

Data are presented as percentages except for AUROC. Data in parentheses are the number of subjects, which was used to calculate the percentage. Data in brackets are 95% confidence intervals. AUROC *p* values indicate the results of the comparisons of AUROC between intrahepatic lipid content and whole hepatic lipid ratio.

AUROC, area under the receiver operating characteristic curve; ^{1}H-MRS, proton magnetic resonance spectroscopy; NAFLD, nonalcoholic fatty liver disease; NPV, negative predictive value; PPV, positive predictive value